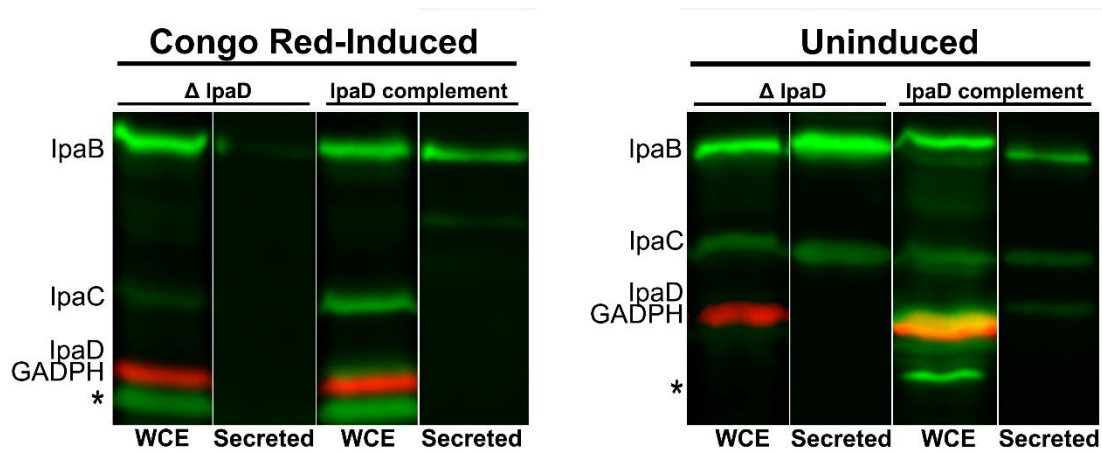


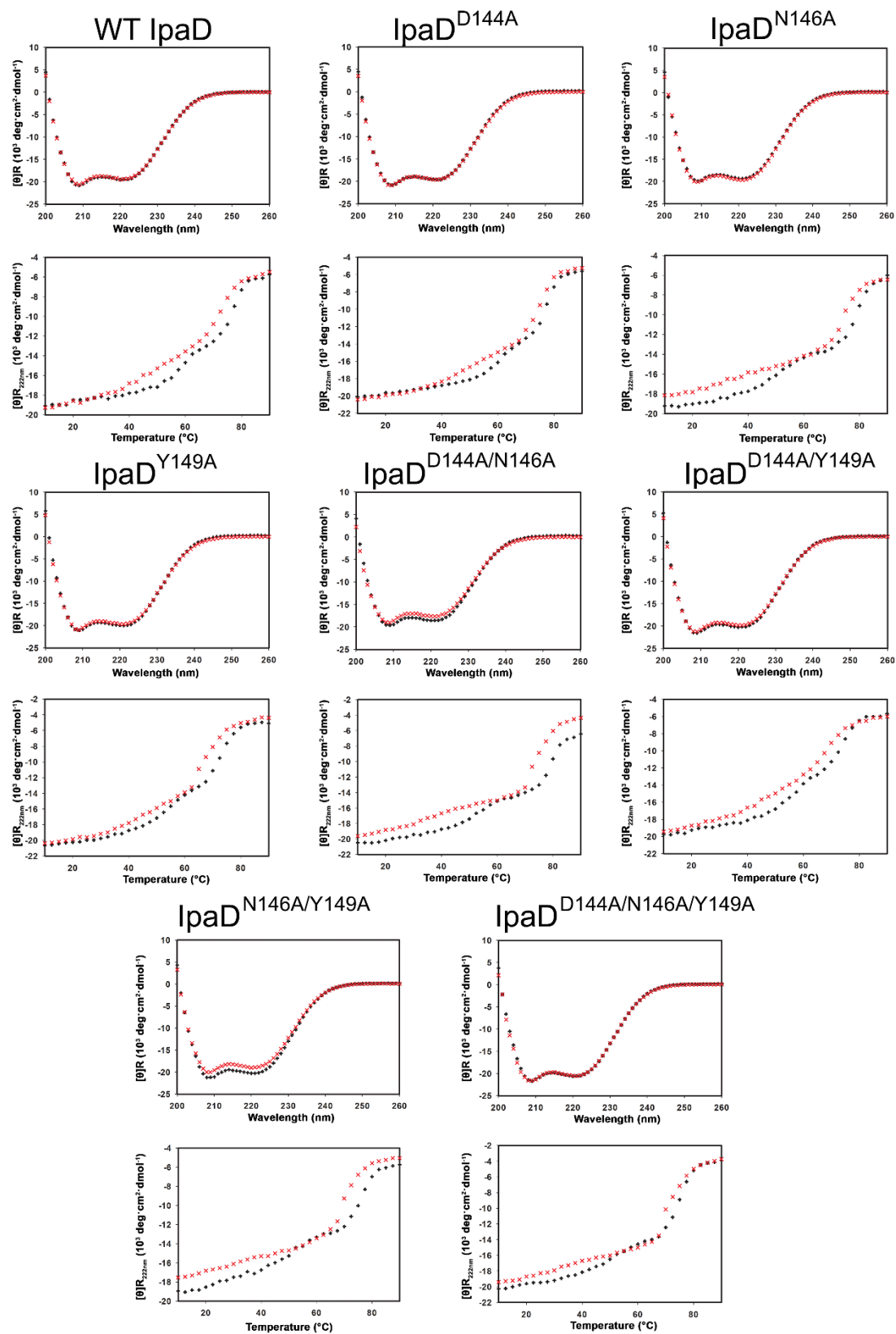
Supporting Information for publication:

**Deoxycholate-Enhanced *Shigella* Virulence is Regulated by a Rare  $\pi$ -Helix in the Type Three  
Secretion System Tip Protein IpaD**

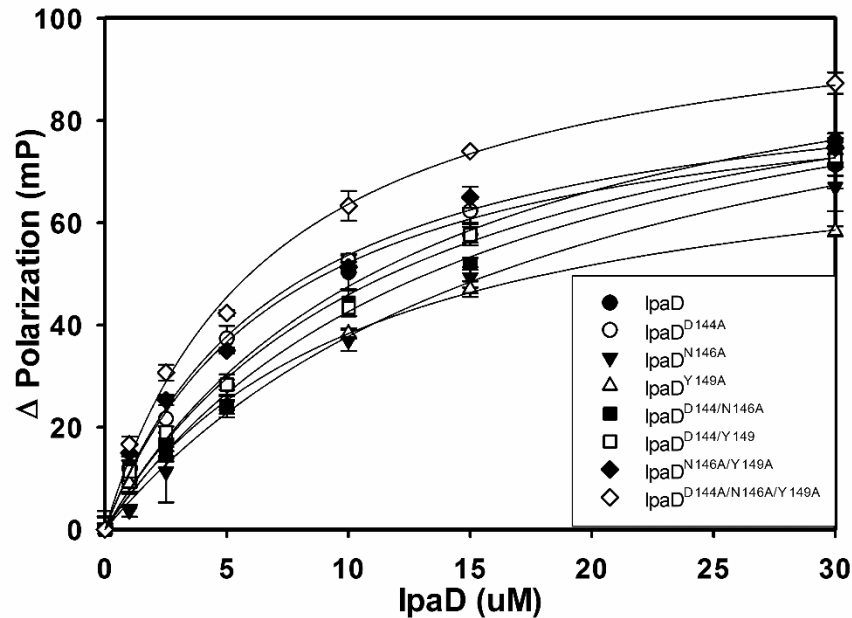
Abram R. Bernard, T. Carson Jessop, Prashant Kumar, and Nicholas E. Dickenson\*



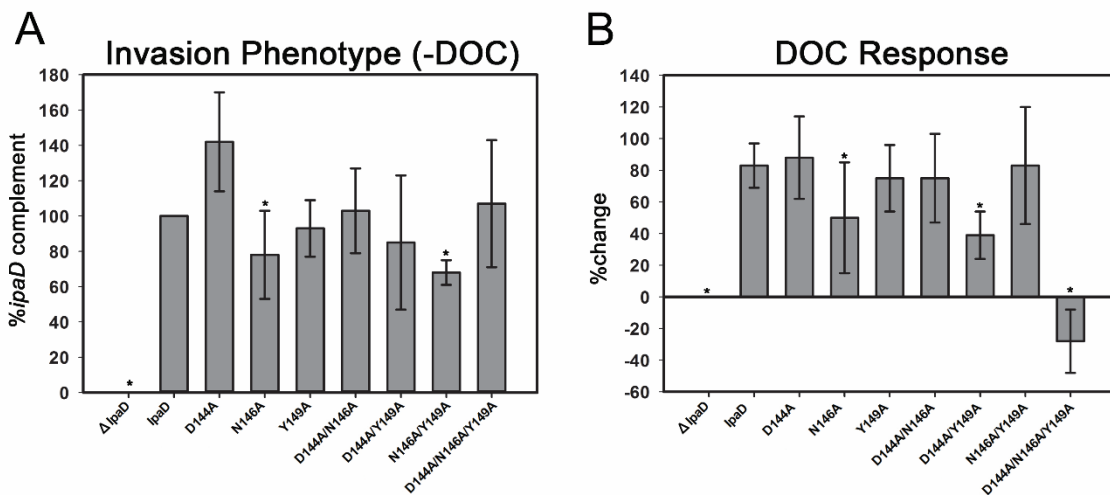
**Supplementary Figure S1: Validation of western blot analysis of uninduced and Congo red-induced *Shigella* secretion profiles.** Polyclonal antibodies against IpaB, IpaC, and IpaD (green) provide a semi-quantitative measure of uninduced overnight protein secretion and Congo red induced protein secretion profiles for both  $\Delta$ IpaD and IpaD complemented *Shigella flexneri* strains. A monoclonal antibody against the cytoplasmic protein glyceraldehyde-3-phosphate dehydrogenase (GADPH) was used as a cytoplasmic control (red). GADPH was detected in the whole cell extract (WCE) of both strains and was not observed in the supernatant, confirming that the T3SS proteins observed in the supernatant were secreted from the bacterial cytoplasm. \* Indicates a cytoplasmic *Shigella* protein with cross reactivity to one of the polyclonal antibodies used in the analysis.



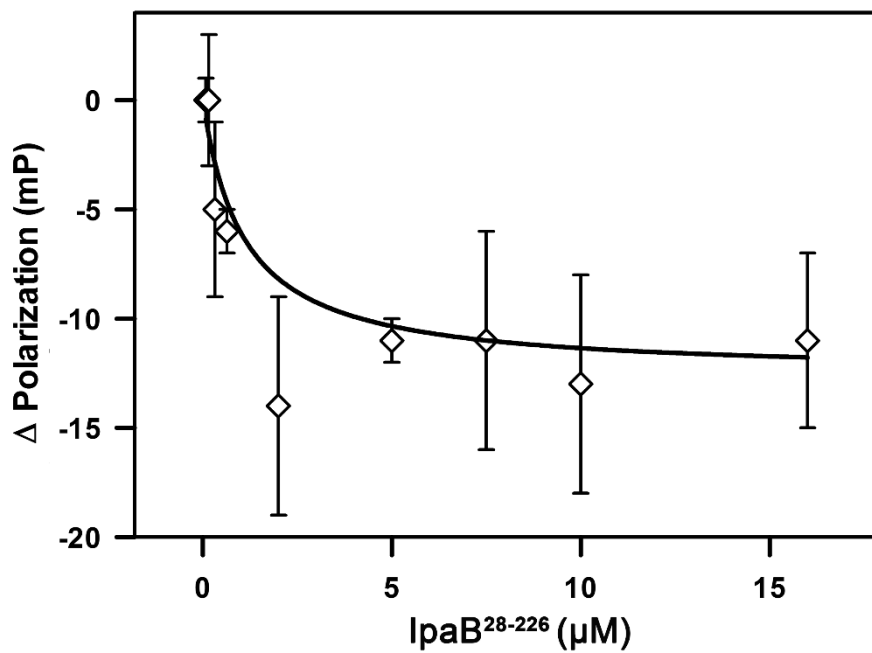
**Supplementary Figure S2: Individual representative CD spectra and thermal transition profiles for wild-type IpaD and each of the seven IpaD  $\pi$ -helix mutants in this study.** Far-UV CD spectra were collected from 200 - 260 nm in the absence (black plus) and presence of 1 mM DOC (red X). Thermal profiles were obtained by measuring CD signal at 222 nm as the protein samples were heated from 10 - 90 °C.



**Supplementary Figure S3: Fluorescence polarization binding curves resulting from interaction between the engineered IpaD constructs and FITC-labeled DOC.** FITC-DOC was maintained at a 25 nM concentration while the concentrations of IpaD ranged from 0 – 30  $\mu\text{M}$ . The polarization data were fit using a single site saturation model to determine an apparent  $K_d$  for each IpaD-DOC interaction. Each curve is generated from triplicate measurements and is then representative of three independent experimental sets.



**Supplementary Figure S4: Invasion phenotypes of *Shigella* strains expressing wild-type IpaD and each of the engineered IpaD  $\pi$ -helix mutants in this study.** **A)** The ability of each of the mutant strains to invade cultured eukaryotic cells is shown relative to the strain expressing wild-type IpaD. **B)** The percent change in invasiveness resulting from exposure to 1 mg/mL DOC is shown for each of the tested strains. Analyses were performed on a minimum of three independent replicates with the results representing the mean  $\pm$  standard deviation. \* Indicates statistical difference from the wild-type IpaD complement strain under identical DOC conditions (one-way ANOVA followed by a Dunnett's post test,  $p \leq 0.01$ ).



**Supplementary Figure S5: Fluorescence polarization competition assay.** 3.5  $\mu\text{M}$  wild-type IpaD was incubated with 80 nM IpaB<sup>28-226</sup>-Alexa586 in the presence of 1 mM DOC. Label free IpaB<sup>28-226</sup> was titrated to a maximum concentration of 16  $\mu\text{M}$ . The observed polarization signal decreased as a function of unlabeled IpaB concentration (fit to a single site saturation model), resulting from the exchange of labeled with unlabeled ligand and confirming a specific interaction between IpaD and IpaB<sup>28-226</sup> that is independent of the conjugated fluorophore. Error bars represent the standard deviation around the mean resulting from three measurements.

## Circular Dichroism Results

IpaD Mutant	Percent secondary structure (% $\pm$ SD)						T <sub>m</sub> ( $^{\circ}$ C $\pm$ SD)	
	-DOC			+DOC			-DOC	+DOC
	$\alpha$ -Helix	$\beta$ -Sheet	Random Coil	$\alpha$ -Helix	$\beta$ -Sheet	Random Coil		
Wild-type IpaD	68 $\pm$ 1	4 $\pm$ 0	28 $\pm$ 1	68 $\pm$ 3	4 $\pm$ 1	28 $\pm$ 2	78.2 $\pm$ 0.2	73.0 $\pm$ 0.3 <sup>‡</sup>
D144A	68 $\pm$ 0	4 $\pm$ 0	28 $\pm$ 0	68 $\pm$ 2	4 $\pm$ 1	28 $\pm$ 1	78.1 $\pm$ 0.3	74.4 $\pm$ 1.0 <sup>‡</sup>
N146A	65 $\pm$ 4	5 $\pm$ 1	29 $\pm$ 2	63 $\pm$ 3	6 $\pm$ 1	31 $\pm$ 2	77.4 $\pm$ 4.5	74.4 $\pm$ 1.1
Y149A	70 $\pm$ 1	3 $\pm$ 1	26 $\pm$ 1	69 $\pm$ 3	4 $\pm$ 1	27 $\pm$ 2	72.7 $\pm$ 0.6	65.2 $\pm$ 0.7 <sup>*‡</sup>
D144A/N146A	67 $\pm$ 4	4 $\pm$ 2	28 $\pm$ 2	64 $\pm$ 4	6 $\pm$ 2	30 $\pm$ 2	78.6 $\pm$ 2.8	74.9 $\pm$ 1.5
D144A/Y149A	74 $\pm$ 4	2 $\pm$ 1	24 $\pm$ 3	70 $\pm$ 3	3 $\pm$ 1	26 $\pm$ 2	74.7 $\pm$ 0.6	70.3 $\pm$ 2.5
N146A/Y149A	68 $\pm$ 2	4 $\pm$ 1	28 $\pm$ 1	62 $\pm$ 2	6 $\pm$ 1	31 $\pm$ 1	76.0 $\pm$ 1.7	70.4 $\pm$ 0.4 <sup>‡</sup>
D144A/N146A/Y149A	68 $\pm$ 2	4 $\pm$ 1	27 $\pm$ 2	65 $\pm$ 5	5 $\pm$ 2	30 $\pm$ 3	76.6 $\pm$ 1.0	71.8 $\pm$ 1.2 <sup>‡</sup>

**Supplementary Table S1: Summary of circular dichroism secondary structure predictions and melting temperatures (T<sub>m</sub>) for wild-type IpaD and the seven  $\pi$ -helix IpaD mutants in the absence and presence of DOC.** Far-UV circular dichroism spectra were obtained for all wild-type and mutant IpaD constructs at 0.3-0.6 mg/mL. The Dichroweb software package K2D was used to analyze secondary structure content. Thermal unfolding profiles were collected by monitoring CD signal at 222 nm as the sample temperature increased from 10  $^{\circ}$ C to 90  $^{\circ}$ C. T<sub>m</sub> values were determined by identifying the inflection point of each major transition to fully unfolded protein. Predicted secondary structure content and T<sub>m</sub> values are reported as a mean value  $\pm$  standard deviation resulting from analysis of at least three independent spectra/profiles per protein. The predicted content of each of the mutants was consistent among groups (one-way ANOVAs) with no significant difference in the predicted structure as a result of DOC exposure (two-tailed Student's t-test,  $p \leq 0.01$ ). \* Indicates statistical difference in T<sub>m</sub> compared to wild-type IpaD under identical DOC conditions (one-way ANOVA followed by a Dunnett's post test,  $p \leq 0.01$ ). ‡ Indicates statistical difference in T<sub>m</sub> compared to the same IpaD construct in the DOC absent condition (2-tailed t-test,  $p \leq .01$ ).

### Uninduced Protein Secretion Profiles

IpaD Mutant	Ratio of Observed Protein (supernatant/pellet)		
	IpaB	IpaC	IpaD
Wild-type IpaD	0.9 ± 0.1	1.6 ± 0.4	1.9 ± 0.4
D144A	1.0 ± 0.2	1.8 ± 0.4	2.2 ± 1.0
N146A	1.3 ± 0.2	1.4 ± 0.2	3.4 ± 0.5
Y149A	1.6 ± 0.5	2.1 ± 0.2	1.9 ± 0.5
D144A/N146A	1.6 ± 0.6	2.9 ± 0.7*	2.2 ± 0.8
D144A/Y149A	0.8 ± 0.2	0.9 ± 0.2	2.3 ± 0.4
N146A/Y149A	1.0 ± 0.1	1.6 ± 0.1	1.8 ± 0.2
D144A/N146A/Y149A	0.8 ± 0.2	1.4 ± 0.3	2.2 ± 0.6

**Supplementary Table S2: Summary of uninduced protein secretion profiles for *Shigella* strains expressing each of the tested IpaD constructs.** The secreted/cytoplasmic ratios of IpaB, IpaC, and IpaD detected by western blot analysis (Figure 3) following overnight growth of the *Shigella* strains expressing the indicated IpaD constructs. The data are presented as mean ± standard deviation resulting from 3 independent experiments. \* Indicates statistical difference in secretion ratio of the specified protein compared to wild-type IpaD (one-way ANOVA followed by a Dunnett's post test,  $p \leq 0.01$ )).